NIH RELAIS Document Delivery

NIH-10286721

JEFFDUYN

NIH -- W1 RA354

JOZEF DUYN
10 Center Dirve
Bldg. 10/Rm.1L07
Bethesda, MD 20892-1150

ATTN:
PHONE: 301-594-7305
FAX: -
E-MAIL:

SUBMITTED: 2002-08-29 17:22:18
PRINTED: 2002-09-03 09:44:57
REQUEST NO.:NIH-10286721
SENT VIA: LOAN DOC
7967430

NIH Fiche to Paper Journal

TITLE: RADIOLOGY
PUBLISHER/PLACE: Radiological Society Of North America Easton Pa
VOLUME/ISSUE/PAGES:1993 Jul;188(1):277-82 277-82
DATE: 1993
AUTHOR OF ARTICLE: Duyn JH; Gillen J; Sobering G; van Zijl PC; Moonen CT
TITLE OF ARTICLE: Multisection proton MR spectroscopic imaging of th
ISSN: 0033-8419
OTHER NOS/LETTERS: Library reports holding volume or year
0401260
8511313
SOURCE: PubMed
CALL NUMBER: W1 RA354
REQUESTER INFO: JEFFDUYN
DELIVERY: E-mail: jhd@helix.nih.gov
REPLY: Mail:

Multisection Proton MR Spectroscopic Imaging of the Brain[1]

Jeffrey H. Duyn, PhD
Joseph Gillen, BS
Geoffrey Sobering, PhD
Peter C. M. van Zijl, PhD
Chrit T. W. Moonen, PhD

The authors developed a hydrogen-1 proton magnetic resonance (MR) imaging method in which metabolic information is acquired by obtaining multiple sections through the brain. A spin-echo sequence is used for section selection, an octangular outer volume saturation pulse for lipid suppression, and a chemical-shift-selective saturation pulse for water suppression. High-quality maps of choline, creatine, and *N*-acetylaspartate were obtained in six studies performed in four volunteers. Water and lipid signal from the skull area was well suppressed by the pulse sequence used.

Index terms: Brain, MR, 15.12145 • Magnetic resonance (MR), spectroscopy, 15.12145

Radiology 1993; 188:277–282

In recent years, there has been increasing interest in the study of brain metabolism with proton magnetic resonance (MR) spectroscopy and spectroscopic imaging, because they allow noninvasive assessment of regional biochemical activity (1–4). Metabolite levels are measured in a single volume with proton spectroscopy; with proton spectroscopic imaging, the spatial distribution of metabolites (*N*-acetylaspartate [NAA], total choline, total creatine, and lactate at an echo time [TE] of 272 msec, for example) is measured over a predetermined volume of interest (VOI). Hydrogen spectroscopic imaging (HSI) studies of diseased brain have shown locally altered metabolite levels in chronic and acute brain infarction (5,6), multiple sclerosis (7,8), epilepsy (9,10), brain tumors (11–13), and acquired immunodeficiency syndrome (14).

Most existing HSI techniques used in evaluating human brain metabolism are based on preselection of a VOI within the skull, to reduce the undesirable resonances of water and lipid originating from areas outside the VOI (15–19). This is generally achieved with a double spin-echo technique (20,21) or a stimulated-echo technique (22–25). One or two dimensions of gradient phase encoding are employed to spatially discriminate within the VOI. Most recently, HSI experiments have been extended to three dimensions of phase encoding (17,26), allowing extension of the VOI in all three dimensions and obtainment of metabolic information from a larger brain volume. Because of the large number of phase-encoding steps in such experiments, the clinical limitation on the total measurement time becomes a severe restriction. For example, an experiment with 16 × 16 × 12 phase-encoding steps and a repetition time (TR) of 2 seconds would require 1.5 hours of total measurement time. In the case of severely ill or unstable patients, such study lengths are prohibitive.

In this work, we present an alternative multisection HSI technique, in which the VOI is allowed to extend closer toward the skull. Preliminary results of this work were recently presented (27), at the same time as an alternative multisection technique (28) in which lipid suppression is achieved on the basis of T1 differences between lipid and metabolites of interest.

Materials and Methods

Subjects.—Six studies were performed in four healthy volunteers (three men and one woman; age range, 25–37 years), all of whom provided informed consent as approved by a National Institutes of Health Intramural Review Board.

MR proton spectroscopic imaging.—All experiments were performed with a conventional 1.5-T whole-body imager (Signa; GE Medical Systems, Milwaukee, Wis) with actively shielded gradients of 10 mT/m strength. The multisection pulse sequence consisted of three parts: (*a*) a chemical shift-selective (CHESS) saturation pulse for water suppression (29–32); (*b*) an outer volume saturation (OVS) pulse for suppression of lipid and water signals originating from the skull and scalp (17); and (*c*) a spin-echo sequence for section selection (27) (Fig 1).

The CHESS sequence (Fig 1a) was a combination of a single-lobe sinc radiofrequency (RF) pulse of 18-msec duration with a gradient crusher pulse of 20-msec duration and 14 mT/m total strength. To avoid unwanted echoes, the direction of the crusher pulse was changed for each acquisition. For each study, the flip angle was adjusted to compensate for T1 relaxation effects (31).

The OVS sequence (Fig 1b) consisted of eight sinc-gauss (four-lobed sinc) section-selective pulses of 4-msec duration and exciting eight sections of 35-mm thickness just outside the brain, along the outline of the skull. The same set of OVS sections was used for each brain section studied. The orientation and position of each of these sections was calculated from coordinates describing the brain outline. The coordinates, four in the superior plane and four in the inferior plane, were measured by the operator from localizer gradient-recalled acquisition in the steady state (GRASS; GE Medical Systems) MR images. The OVS sections generally tilted toward the caudocranial axis. The RF pulses were applied in four pairs, each pair followed by an 8-msec crusher gradient pulse of 14 mT/m. The pulse pairs selected pairs of opposing sections (left and right, anterior and posterior, and the two diagonal pairs) as indicated in Figure 1c. The crusher orientation was changed for subsequent pulse pairs, to avoid unwanted echoes. The flip angle of each RF pulse was corrected for T1 relaxation effects (31), with the assumption that lipid T1 was 280 msec.

The spin-echo sequence (Fig 1a) consisted of a section-selective 90° and a 180° RF pulse exciting approximately the same section. The 180° RF pulse was flanked by 4-msec gradient crushers in the x, y, and z directions, resulting in strength of 17 mT/m. The crusher orientation was changed for each section, to avoid unwanted echoes. The nominal section thickness was 13 mm. The bandwidth of the 90° pulse was 2.0 kHz. The bandwidth of the numerically optimized 180° RF pulse was slightly larger (2.2 kHz), to improve the section profile. A 256-msec echo was acquired symmetrically at a TE of approximately 272 msec. The spectral width was 1,000 Hz.

Four axial or oblique (anterior-posterior angulation) parallel sections were excited sequentially by changing the

[1] From the Laboratory of Diagnostic Radiology Research (J.H.D.) and the In Vivo NMR Research Center (J.H.D., G.S., C.T.W.M.), National Institutes of Health, Bldg 10, Room B1D-125, Bethesda, MD 20892; Pittsburgh NMR Institute, Pittsburgh, Pa (J.G.); and the Russell H. Morgan Department of Radiology and Radiological Sciences, The Johns Hopkins Medical Institutions, Baltimore, Md (P.C.M.v.Z.). Received December 10, 1992; revision requested February 2, 1993; revision received February 18; accepted February 23. **Address reprint requests to** C.T.W.M.

transmitter frequency offset for both 90° and 180° RF pulses. With an intersection gap of 4.5 mm, there was negligible overlap between sections. Therefore, magnetization of a specific section was not perturbed while other sections were studied. An effective TR of 2.3 seconds was used. Water and OVS suppression were independent of the particular section being studied. The sections were studied in consecutive order, starting from the most inferior location. Two-dimensional phase encoding was performed immediately following application of the last gradient crusher pulse, prior to data acquisition (18). Thirty-two by 32 phase-encoding steps were used over a 240-mm field of view. A circular k-space sampling scheme (33) reduced the total number of phase-encoding steps by 25%, for a total acquisition time of 27 minutes.

Protocol.—Prior to the HSI experiment, sagittal GRASS images were acquired and used to determine position and angulation of the VOI. Subsequently, multiple (5-mm-thick) GRASS MR images were obtained at 600/30 (TR msec/TE msec) at the predetermined angulation, with a flip angle of 30°. The most inferior HSI section was chosen to be just above the sinuses. The coordinates for positioning the OVS pulses were measured from the oblique GRASS images. Subsequently, the multisection spectroscopy sequence was run in single-section mode, to adjust the power output of the RF amplifier and to optimize the homogeneity of the constant magnetic induction field (B_0). For this purpose, the section thickness was set to 65 mm to encompass all of the volume to be studied, and the OVS pulses were switched off. The RF power was adjusted by maximizing the spin-echo signal. Finally, the RF pulse angle of the CHESS water suppression pulse was optimized, and the HSI experiment was begun. After completion, a series of oblique GRASS MR images was obtained at 600/30 with a flip angle of 30° and a section thickness and location corresponding with that used in acquisition of the spectroscopic images. The total study time, including setup, MR imaging, and HSI data acquisition, was less than 1 hour.

Data processing.—The raw data matrix of 256 × 32 × 32 × 4 quadrature pairs was transferred to a workstation (Sun Microsystems; Mountain View, Calif) for off-line processing and viewing by means of software developed with the IDL data processing language (Research Systems, Boulder, Colo). Each section was then processed separately. First, cosine filters were applied in the spectral and spatial domains. The spatial filter was applied radially (two-dimensional filter), starting at half the maximum radius. The data matrix for each

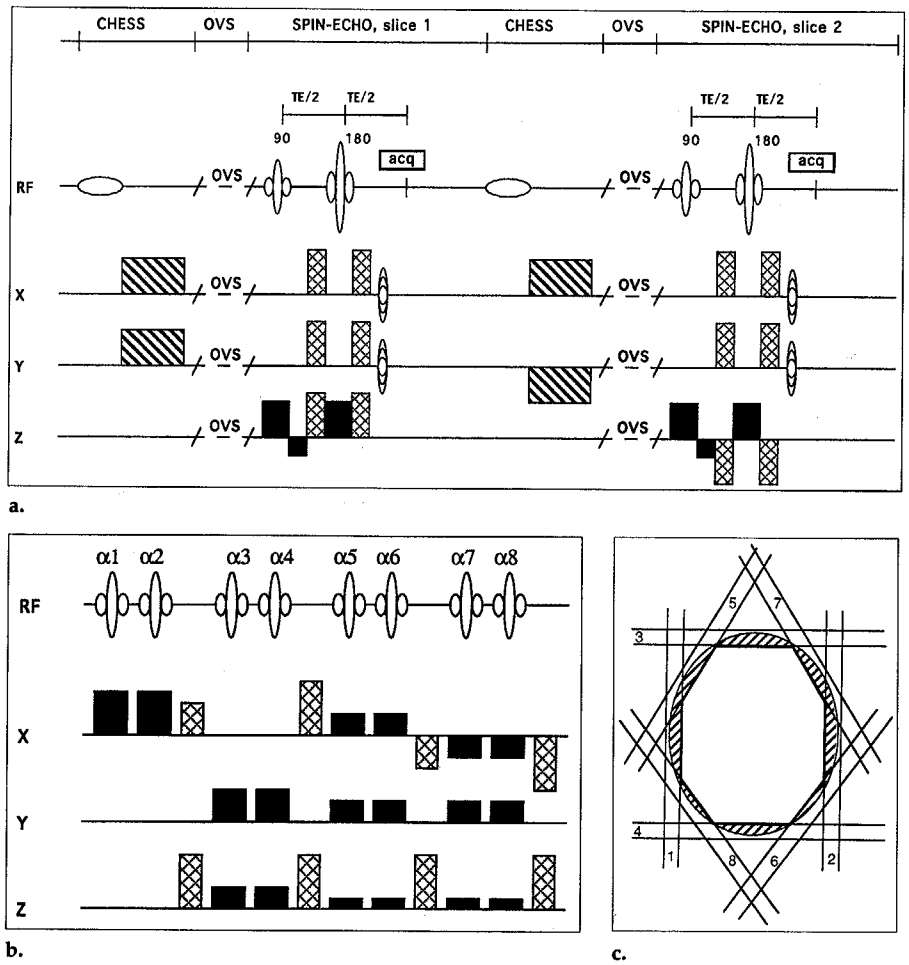

Figure 1. Pulse sequence diagrams for multisection proton spectroscopic imaging. Gradient crushers (▨) and section-selection gradients (■) are indicated. **(a)** Basic spin-echo sequence for section selection. A CHESS pulse for water suppression is included. Gradient crushers for phase dispersion of the water magnetization are indicated (▨). The frequencies of both section-selection RF pulses are changed for each consecutive section. The diagram covers two sections. Notice the change in direction of the TE crushers and water suppression gradients to avoid unwanted echoes. The acquisition window is shortened for clarity. The timing of the OVS pulse is indicated. *acq* = acquisition. **(b)** OVS scheme for suppression of eight sections around the brain. The OVS is arranged in four pairs of opposite sections, each pair followed by a crusher gradient. Flip angles are indicated as separate α pulses (α > 90°) to indicate the small differences to adjust for T1 relaxation of lipid resonances. **(c)** Order and location of the sections (points *1–8*) of the OVS suppression.

section was zero-filled to 512 × 64 × 64 points, and three-dimensional Fourier transformation was performed. The resulting effective in-plane spatial resolution was 12 mm, as calculated from the contour of the two-dimensional point spread function at half maximum height, including a correction for effects of the circular k-space sampling scheme. Spectra were corrected for B_0 inhomogeneities by referencing to the position of NAA. If the NAA intensity dropped below a certain threshold, its position was copied from neighboring voxels. Metabolite images of NAA, choline, and creatine were created by integrating metabolite peaks over a frequency band of 0.18 ppm.

Since lipid and water suppression are crucial markers of HSI performance, both were evaluated by using an automated analysis of all spectra, originating from regions within the area suppressed by the OVS pulses. In this analysis, the spectral regions from 1.70 to 1.88 ppm and from 2.24 to 2.42 ppm (upfield and downfield from NAA, respectively) were regarded as representative of lipid contamination, whereas the spectral area from 3.40 to 3.58 ppm (downfield from choline) was regarded as representative of water contamination. A measure of contamination was obtained by integrating all spectra in these spectral areas and normalizing to the NAA intensity.

Results

Figure 2 shows four consecutive planes (inferior to superior) from an HSI study obtained in a healthy volun-

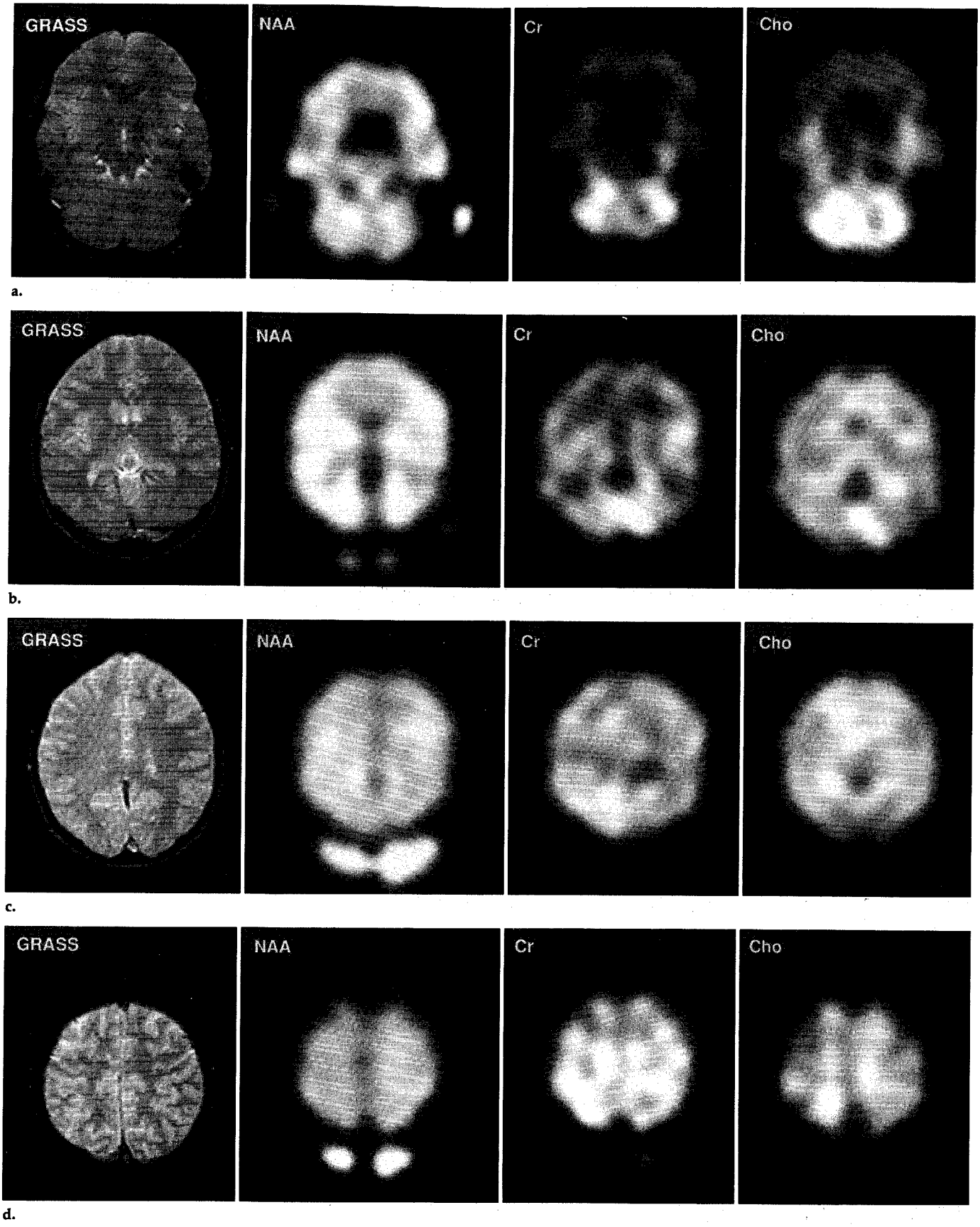

Figure 2. Multisection HSI data set of the brain of a healthy volunteer shows four parallel oblique (20°) sections (13-mm thickness, 4.5-mm gap). The order **(a–d)** is from inferior to superior. For each section, a GRASS image (600/30; flip angle, 30°) and maps of total creatine (*Cr*), total choline (*Cho*), and NAA are shown. Image intensity is linear from zero to the maximum level. Notice the drastic increase in choline and creatine levels in the cerebellum compared within the remainder of the section, and the loss of metabolite intensity in the ventricles and middle portion of the brain, accurately corresponding to the GRASS images. No lactate was detected. On the NAA images, the hyperintense spots outside the brain resulted from residual lipid signal.

teer. For each plane, a GRASS image and NAA, choline, and creatine metabolite maps are given. The intensity scaling is adjusted for each image. The increased choline and creatine in gray matter of the cerebellum and the signal losses in cerebrospinal fluid spaces anterior to the cerebellum and near the caudate nuclei and globi pallidi are clearly seen in section 1 (Fig 2a). The signal loss in the caudate nuclei and globi pallidi is possibly due to susceptibility effects. In section 2 (Fig 2b), the creatine signal is reduced in white matter. In all sections, the major cerebrospinal fluid spaces (ventricles and midline) are easily identified from signal loss of the metabolites, demonstrating the excellent HSI quality. The signal-to-noise ratio for the NAA images varies between 15 and 20. All six studies performed in the volunteers were successful.

An example of the analysis of lipid contamination is shown in Figure 3 as a histogram of the number of volume elements (in percentage of the total number of brain voxels) containing "lipid" intensity (in percentage of the NAA intensity). The solid curve shows a symmetrical distribution, centered around 9%. This indicates almost complete elimination of lipid contamination because the value of 9% is close to the noise level. To evaluate the effects of the OVS procedure, the experiment was repeated without OVS. This experiment is represented by the dashed curve, showing a relatively broad distribution and reaching a maximum at about 20%, indicating substantial lipid contamination.

The results of the contamination analysis performed in all studies are averaged over all four planes and summarized in the Table. The contamination of water and lipid is each characterized in the Table by three numbers: the distribution maximum and width and the number of spectra with a contamination exceeding 20%. The distribution of both water and lipid contamination was similar to the distribution given by the solid curve of Figure 3. In all studies, the lipid contamination was slightly larger than the water contamination. In none of the studies did the distribution maximum exceed 10%. The number of spectra with contamination exceeding 20% was 1.3% for water and 5.9% for lipid (mostly close to the skull), averaged over all studies. Study 4 had an exceptionally large number of spectra (15.3%) with a lipid contamination exceeding 20%. Reexamination of the experimental parameters showed an operator error in the positioning of the OVS pulses.

Another demonstration of the effects of the OVS procedure on the spectral quality is presented in Figure 4. An array of spectra is shown from a region in the right occipital brain through the skull. The upper two rows of spectra were obtained from a multisection HSI study with OVS, and the lower two rows of spectra, from a multisection HSI spectroscopic study without OVS. With OVS, the suppression of lipid signal is 90% or better in spectra from the skull area. More important, the beneficial effect of OVS is clearly seen in other areas remote from the skull. This is because the large unsuppressed lipid resonances can bleed into the spectra of brain regions, partly from the shape of the point spread function being less than ideal and partly from patient motion. The latter effect seems to be the largest, since the lipid contamination does not decrease with distance from the skull.

Summary of Analysis of Water and Lipid Contamination in All Brain Spectra Obtained with Multisection HSI Combined with OVS in Six Volunteers

	Water Contamination		Lipid Contamination	
Study No.	Average (%)*	Percentage of Voxels with Contamination >20%†	Average (%)*	Percentage of Voxels with Contamination >20%†
1	6.8 (4.3)	2.2	7.8 (4.3)	1.4
2	8.0 (5.5)	0.5	9.3 (4.5)	7.2
3	5.4 (4.3)	0.2	9.3 (5.3)	5.1
4	6.8 (6.0)	2.4	9.3 (4.8)	15.3
5	5.5 (4.0)	0.2	8.0 (5.7)	3.3
6	7.7 (6.3)	2.0	8.3 (5.0)	3.0

Note—Contaminations are expressed as percentages of the maximum integrated NAA resonance.
* Average water and lipid contamination values were determined from the peak positions in the respective contamination histograms (Fig 3). The noise level (no contamination) is about 6.0 for the signal-to-noise ratio obtained in these studies. Values in parentheses represent the width at half the height of the histogram peak.
† Indicated are the number of voxels (as percentage of the total number of brain voxels) containing a water-lipid signal intensity above a threshold of 20% of the maximum integrated NAA resonance.

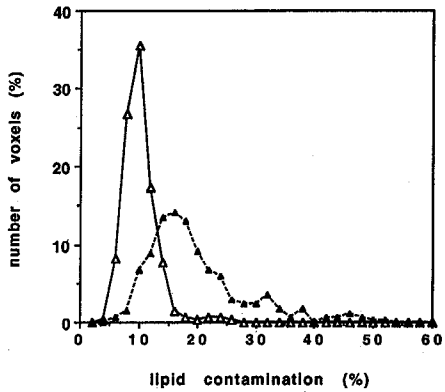

Figure 3. Comparison of lipid contamination with OVS (△) and without OVS (▲). The histogram shows the percentage of voxels of the brain as a function of the lipid contamination. The units of contamination are given as a percentage of the maximum integrated NAA intensity. The noise level is at about 6%. Values were obtained from the most inferior section (including cerebellum, upper brainstem, and cerebrum just above the sinuses) from a study of four sections.

Discussion

A multisection approach allows simultaneous acquisition of multiple sections without a time, resolution, or signal-to-noise penalty. This is made possible by using a simple spin-echo sequence that excites magnetization in only the section under study. This is unlike conventional VOI preselection, which is based on sequential excitation of orthogonal planes, perturbing the magnetization in all sections. A problem with single-section excitation without volume preselection in all dimensions is the bleed of lipid from skull into brain spectra (27). To avoid this, outer volume suppression is employed prior to the HSI sequence.

The combination of consecutive single-section excitation and OVS has additional advantages. The HSI spin-echo sequence achieves slightly higher signal-to-noise ratio for the metabolites, because only one RF refocusing pulse is used. In addition, motion sensitivity is decreased. This is due to the substantially decreased gradient crushers around the remaining refocusing pulse as compared with the conventional method (27). With our method, the same single section is excited by both 90° and 180° RF pulses and thus, less unwanted magnetization has to be dephased. We also found that water suppression is superior to that obtained with previous methods of ours, performed with hardware identical to that used in this study. This improved performance is attributed to the following: First, water signal from skull areas, which is difficult to saturate with the CHESS sequence because of susceptibility effects, is partially suppressed by the OVS sequence; second, the repetitive, single-section excitation without volume preselection avoids excitation of water outside the VOI; third, water suppression is repeated for each section but affects water in all sections, leading to an effective TR shorter than the T1 of water, thereby providing some addi-

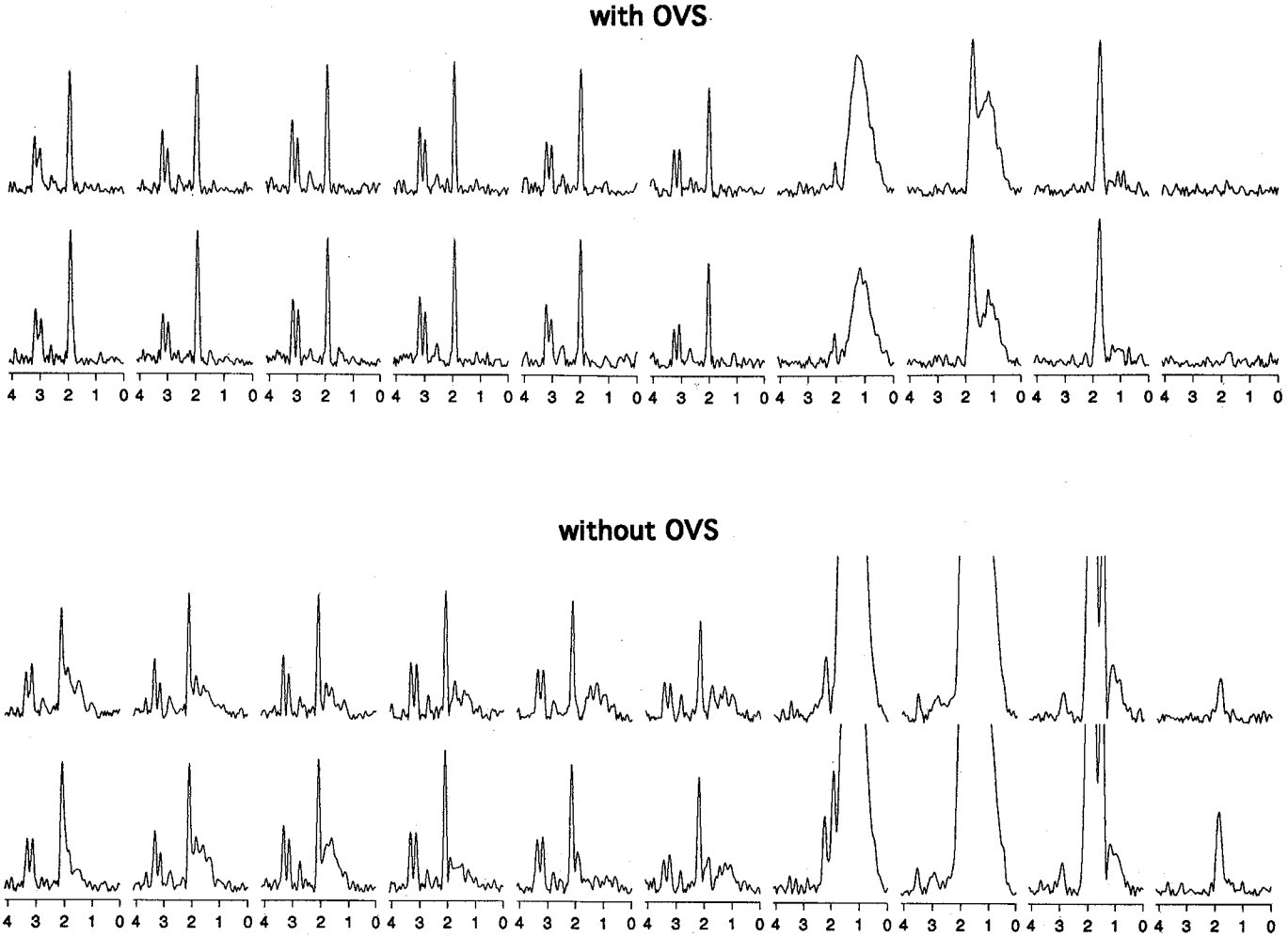

Figure 4. Array of spectra (magnitude mode) from an area in the occipital region including the skull, obtained with OVS (upper two rows) and without OVS (lower two rows). Resonances in brain spectra (left four spectra in each row) are easily recognized at 2.0 ppm (NAA), 3.0 ppm (total creatine), and 3.2 ppm (choline). Strong lipid resonances are seen without OVS in the skull region. Notice the effective suppression with OVS and the resulting reduction in lipid bleeding into the brain spectra and into the "empty" region represented by the spectra on the right.

tional water suppression due to saturation effects. As a consequence, there was no need to apply postprocessing water suppression (34).

In conclusion, multisection spin-echo HSI combined with OVS for lipid suppression and with frequency-selective water suppression effectively increases the information density of single-section HSI in a clinically feasible measurement time. This robust sequence has several additional advantages compared with conventional methods: improved water and lipid suppression, less motion artifact, improved performance close to the skull, and improved signal-to-noise ratio. ■

Acknowledgments: We thank Joseph A. Frank, MD, for support and discussions; Mark Armstrong, MD, for helpful feedback and interest; and Chris Hardy, PhD, of GE Medical Systems for the optimized refocusing pulses. Denise Sobering is acknowledged for help in the preparation of manuscript and figures.

References

1. Hanstock CC, Rothman DL, Prichard JW, Jue T, Shulman RG. Localized ^{1}H spectra of metabolism in human brain. Proc Natl Acad Sci 1988; 85:1821–1825.
2. Frahm J, Bruhn H, Gyngell ML, Merboldt KD, Haenicke W, Sauter R. Localized high resolution proton NMR spectroscopy using stimulated echoes: initial applications to human brain *in vivo*. Magn Reson Med 1989; 9:79– 93.
3. Luyten PR, Marien AJH, Heindel W, et al. Metabolic imaging of patients with intracranial tumors: H-1 MR spectroscopic imaging and PET. Radiology 1990; 176:791–799.
4. Moonen CTW, van Zijl PCM, Frank JA, Le Bihan D, Becker ED. Functional magnetic resonance imaging in medicine and physiology. Science 1990; 250:53–61.
5. Luyten PR, van Ryen PC, Tulleken CAF, den Hollander JA. Metabolite mapping using ^{1}H NMR spectroscopic imaging in patients with cerebrovascular disease (abstr). In: Book of abstracts: Society of Magnetic Resonance in Medicine 1989. Berkeley, Calif: Society of Magnetic Resonance in Medicine, 1989; 452.
6. Duyn JH, Matson GB, Maudsley AA, Hugg JW, Weiner MW. Human brain infarction: proton MR spectroscopy. Radiology 1992; 183:711–718.
7. Arnold DL, Matthews PM, Francis G, Antel J. Temporal profile of regional chemical-pathological changes in demyelinating lesions defined by MRSI (abstr). In: Book of abstracts: Society of Magnetic Resonance in Medicine 1991. Berkeley, Calif: Society of Magnetic Resonance in Medicine, 1991; 80.
8. Husted CA, Hugg JW, De Bie SH, et al. 1H and 31P spectroscopic imaging (MRSI) of multiple sclerosis (abstr). In: Book of abstracts: Society of Magnetic Resonance in Medicine 1991. Berkeley, Calif: Society of Magnetic Resonance in Medicine, 1991; 83.
9. Luyten PR, van Ryen PC, Meinert LC, Marien AJH, den Hollander JA. Identifying epilepsy (abstr). In: Book of abstracts: Society of Magnetic Resonance in Medicine 1990. Berkeley, Calif: Society of Magnetic Resonance in Medicine, 1990; 1009.
10. Hugg JW, Laxer KD, Matson GB, Maudsley AA, Weiner MW. ^{1}H MR spectroscopic imaging detects neuronal loss more sensitively than MRI in focal epilepsy (abstr). In: Book of abstracts: Society of Magnetic Resonance in Medicine 1992. Berkeley, Calif: Society of Magnetic Resonance in Medicine, 1992; 1913.
11. Segebarth CM, Baleriaux DF, Luyten PR, den Hollander JA. Detection of metabolic heterogeneity of human intracranial tumors in vivo by 1H NMR spectroscopic imaging. Magn Reson Med 1990; 13:62–76.
12. Herholz K, Heindel W, Luyten PR, et al. In-vivo imaging of glucose consumption and lactate concentration in human gliomas. Ann Neurol 1992; 31:319–327.
13. Fulham MJ, Bizzi A, Dietz MJ, et al. Map-

ping of brain tumor metabolites with proton MR spectroscopic imaging: clinical relevance. Radiology 1992; 185:675–686.
14. Meyerhoff DJ, Duyn JH, Bachman L, Fein G, Weiner MW. Alterations of brain proton metabolites in HIV infection: preliminary ^{1}H SI findings (abstr). In: Book of abstracts: Society of Magnetic Resonance in Medicine 1991. Berkeley, Calif: Society of Magnetic Resonance in Medicine, 1991; 404.
15. Lampman DA, Murdoch JB, Paley M. In vivo proton metabolite maps using the MESA 3D technique. Magn Reson Med 1991; 18:169–180.
16. Spielman D, Pauly J, Macovski A, Enzmann D. Spectroscopic imaging with multidimensional pulses for excitation: SIMPLE. Magn Reson Med 1991; 19:67–84.
17. Duyn JH, Matson GB, Maudsley AA, Weiner MW. 3D phase encoding ^{1}H spectroscopic imaging of human brain. Magn Reson Imaging 1992; 10:315–319.
18. Moonen CTW, Sobering G, van Zijl PCM, Gillen J, von Kienlin M, Bizzi A. Proton spectroscopic imaging of human brain. J Magn Reson 1992; 98:556–575.
19. Posse S, Schuknecht B, Smith ME, et al. Short-echo-time proton spectroscopic imaging using stimulated echoes and outer volume presaturation. J Comput Assist Tomogr 1992; 17:1–14.
20. Ordidge RJ, Bendall MR, Gordon RE, Connely A. Volume selection for in-vivo spectroscopy. In: Govil G, Khetrapal CL, Saran A, eds. Magnetic resonance in biology and medicine. New Delhi, India: Tata-McGraw-Hill, 1985; 387–397.
21. Bottomley PA. Spatial localization in NMR spectroscopy in vivo. Ann NY Acad Sci 1987; 508:333–348.
22. McKinnon G. Volume selective excitation spectroscopy using the stimulated echo (abstr). In: Works in progress: Society of Magnetic Resonance in Medicine 1986. Berkeley, Calif: Society of Magnetic Resonance in Medicine, 1986; 168.
23. Granot J. Selected volume excitation using stimulated echoes (VEST): applications to spatially localized spectroscopy and imaging. J Magn Reson 1986; 70:488–492.
24. Kimmich R, Hoepfel D. Volume-selective multipulse spin echo spectroscopy. J Magn Reson 1987; 72:379–384.
25. Frahm J, Merboldt KD, Haenicke W. Localized proton spectroscopy using stimulated echoes. J Magn Reson 1987; 72:502–508.
26. Moonen CTW, Sobering G, van Zijl PCM, Gillen J, Daly P. Clinically feasible, short echo time spectroscopic imaging in three dimensions (abstr). In: Book of abstracts: Society of Magnetic Resonance in Medicine 1990. Berkeley, Calif: Society of Magnetic Resonance in Medicine, 1990; 139.
27. Moonen CTW, van Zijl PCM, Gillen J, Sobering G. Multislice proton spectroscopic imaging of the human brain (abstr). In: Book of abstracts: Society of Magnetic Resonance in Medicine 1992. Berkeley, Calif: Society of Magnetic Resonance in Medicine, 1992; 931.
28. Spielman D, Pauly JM, Macovski A, Glover G, Enzmann DR. Lipid-suppressed single- and multisection proton spectroscopic imaging of the human brain. JMRI 1992; 2:253–262.
29. Haase A, Frahm J, Haenicke W, Matthaei D. 1H NMR chemical shift selective (CHESS) imaging. Phys Med Biol 1985; 30:341–344.
30. Doddrell DM, Galloway GJ, Brooks WM, et al. Water signal elimination in vivo, using "suppression by mistimed echo and repetitive gradient episodes." J Magn Reson 1986; 70:176–180.
31. Moonen CTW, van Zijl PCM. Highly effective water suppression for in vivo proton NMR spectroscopy (DRYSTEAM). J Magn Reson 1990; 88:28–41.
32. Van Zijl PCM, Moonen CTW. Solvent suppression strategies for in-vivo NMR. In: Diehl P, Fluck E, Günther H, Kosfeld R, Seelig J, eds. NMR, basic principles and progress 26. Berlin, Germany: Springer-Verlag, 1992; 67–108.
33. Maudsley AA, Hugg JW, Fernandez EJ, Matson GB, Weiner MW. Application of reduced k-space sampling in spectroscopic imaging (abstr). In: Book of abstracts: Society of Magnetic Resonance in Medicine 1991. Berkeley, Calif: Society of Magnetic Resonance in Medicine, 1991; 186.
34. Sobering G, von Kienlin M, Moonen CTW, van Zijl PCM, Bizzi A. Post acquisition reduction of water signals in proton spectroscopic imaging of the brain (abstr). In: Book of abstracts: Society of Magnetic Resonance in Medicine 1991. Berkeley, Calif: Society of Magnetic Resonance in Medicine, 1991; 771.